Mode-locked operation of a diode-pumped femtosecond Yb:SrF_2 laser

F. Druon,[1,*] D. N. Papadopoulos,[1] J. Boudeile,[1] M. Hanna,[1] P. Georges,[1] A. Benayad,[2] P. Camy,[2] J. L. Doualan,[2] V Ménard,[2] and R. Moncorgé[2]

[1]*Laboratoire Charles Fabry de l'Institut d'Optique, CNRS, Université Paris-Sud, RD 128 Campus Polytechnique, 91127 Palaiseau, France*

[2]*Centre de Recherche sur les Ions les Matériaux et la Photonique, UMR 6252 CNRS-CEA-ENSICAEN, Université de Caen, 14050 Caen, France*

**Corresponding author: frederic.druon@institutoptique.fr*

Received May 14, 2009; accepted June 10, 2009;
posted June 26, 2009 (Doc. ID 111303); published July 30, 2009

Femtosecond mode-locked operation is demonstrated for the first time, to our knowledge, with a Yb:SrF_2 crystal. The shortest pulse duration is 143 fs for an average power of 450 mW. The highest average power is 620 mW for a pulse duration of 173 fs. Since Yb:SrF_2 corresponds to the longest-lifetime Yb-doped crystal with which the mode-locking operation has been achieved, a detailed analysis is carried out to characterize the quality of the solitonlike regime. © 2009 Optical Society of America

OCIS codes: 140.3615, 140.4050, 320.7090.

Since the first demonstration, in 2004, of diode-pumped laser operation of Yb-doped calcium fluoride (CaF_2, also known as fluorite or fluorospar) [1], some interest of the laser community has been raised for this crystal and its isotypes: SrF_2 or BaF_2. Actually, this family of crystals has been demonstrated to be a very good candidate for the development of diode-pumped femtosecond lasers [2] with, for example, the recent development of a terawatt chain [3,4]. Three main reasons can explain this trend. First, fluoride isotypes are simple cubic crystals whose crystallographic properties are fairly well known [5]. These crystals can be grown in a large dimension, and optical-quality ceramics have been demonstrated for a very long time. Second, the simple structure of these crystals imparts advantageous thermal properties such as good thermal conductivities, which are of the order of 10 W/m/K for undoped crystals [6,7]. Finally, fluorides have very broad and smooth emission bands [8], which is exceptional for cubic crystals. This is explained by the different valencies of the dopant (Yb^{3+}) and the substituted alkaline cations (Ca^{2+},Sr^{2+},Ba^{2+}), inducing clusters during the doping process [5,9]. This makes them particularly attractive for femtosecond laser development. In terms of high-average-power diode-pumped laser development, Yb:CaF_2 has demonstrated some advantages [6]. The thermal properties for Yb:SrF_2, respectively, (Yb:CaF_2) are 3.6 W/m/K (6.1 W/m/K) for the thermal conductivity of a 2.5% Yb-doped crystal and -18×10^{-6} K^{-1} (-20×10^{-6} K^{-1}) for the thermo-optic coefficient. However, some features are more favorable in the case of the isotype SrF_2, such as a large-absorption cross section around 980 nm and a smooth-gain cross section spectrum (Fig. 1) and others in the case of CaF_2 such as better thermal properties. Another difference between Yb:CaF_2 and Yb:SrF_2 consists of a longer exited-state lifetime for Yb:SrF_2. In fact, with a lifetime of 2.9 ms Yb:SrF_2 has one of the longest lifetimes ever reported for a Yb-doped laser crystal. This is very attractive for storing energy laser amplification, for instance [10]. In counterpart a very long lifetime makes mode-locking (ML) operation more difficult to achieve owing to *Q*-switching (QS) concern [11]. In this Letter we report the first diode-pumped femtosecond oscillator based on Yb:SrF_2 crystal.

The experiment is performed with a 6.1-mm-long 4 mm$\times$7 mm section Brewster-cut Yb:SrF_2 crystal doped at 2.9%. The cavity is presented in Fig. 2 and is very similar to the one described in [12]. The laser diode emits 7 W at 976 nm (3 nm FWHM) out of a 50 μm diameter fiber (NA=0.22). To initiate the ML regime, a semiconductor saturable absorber mirror (SESAM) manufactured by Batop GmbH (SAM-294-II; 23,1045 nm; 1%) is inserted, with the following characteristics: 1% saturable absorption, 1045 nm for the center wavelength, 70 $\mu J/cm^2$ saturation fluence, and incident laser beam waist of 20 μm. The mirrors of the cavity are specified to introduce a low group-velocity delay. The dispersion of the cavity is adjusted by a pair of SF10 prisms nominally separated by 310 mm.

The shortest pulses obtained with this setup have a duration of 143 fs for a 8.5 nm bandwidth spectrum centered at 1046.7 nm. The corresponding average

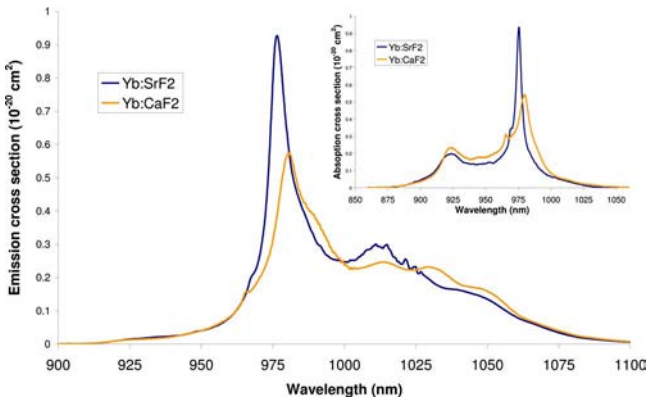

Fig. 1. (Color online) Compared emission and absorption (inset) spectra of Yb:SrF_2 and Yb:CaF_2.

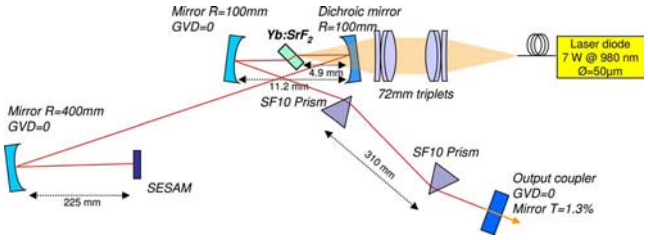

Fig. 2. (Color online) Experimental setup.

power is 450 mW at a repetition rate of 112.5 MHz. The long lifetime of $Yb:SrF_2$ does not favor the mode-locked operation [11], and a solitonlike regime [13] strongly assisted by SESAM [14] is then expected. Soliton and gain filtering play a major role in the ML regime stabilization. Therefore a small deviation from the ideal soliton regime would result in a energy shedding to continuum, which initiates Q-switched operation for this long-lifetime material. In other words, one can then assume that only an "ideal" solution of the unperturbed Haus's master equation [13,15] is stable enough to maintain ML within these nonfavorable conditions. To verify this idea, second-harmonic generation frequency-resolved optical gating (SHG FROG) measurement was performed. One can observe in Fig. 3 that the intensity profile and the flat phase are very close to the soliton solution. Actually, this flat phase brings to a temporal Strehl ratio comparable with the ideal flat-phase sech^2 solution by 98%. This ideal shape is even more obvious in Fig. 4, where the spectral and temporal profiles are plotted in a logarithmic scale. The time–bandwidth product also reflects this closeness to the ideal soliton operation with a value of only 5% above the theoretical value. Moreover, one can notice that, unlike in [12] where the laser operated at the edge of cavity stability to enhance Kerr lens mode-locking (KLM) assistance (which was obvious on the spatial profiles), no spatial modification clearly appears in the present case (Fig. 5) between the cw ML and the Q-switched regimes, clearly indicating the major influence of the SESAM on the ML process. The threshold of mode-locked regime is observed for an average power of 360 mW (Fig. 6); out of the ML regime range, the only observed laser operation is QS.

Another femtosecond regime with more average power and a longer pulse duration is also obtained with the same cavity but operates with a different laser spot location on the SESAM. In this case, 620 mW

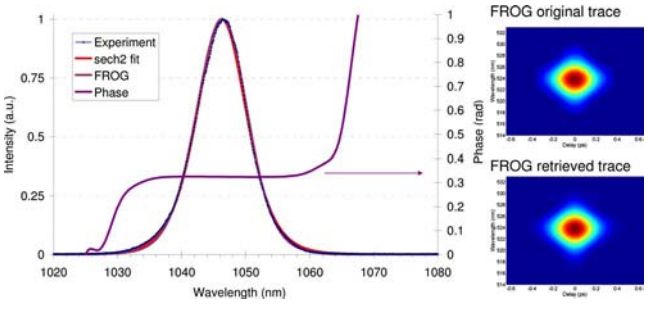

Fig. 3. (Color online) Spectra (left) and spectral phase for the 143 fs pulses directly measured with a spectrometer, retrieved from a SHG FROG (right) and fitted.

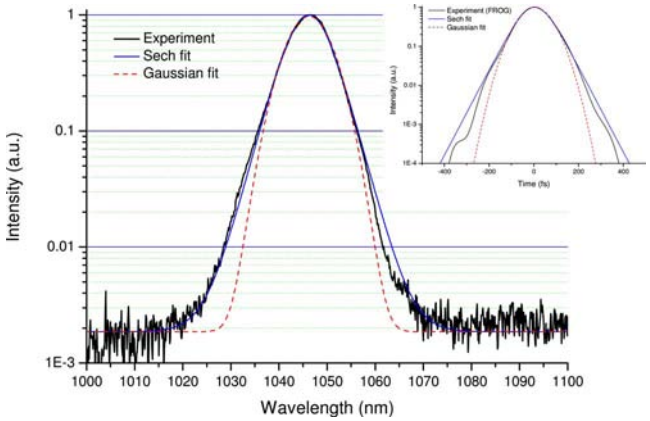

Fig. 4. (Color online) Spectrum and temporal shape comparisons with the sech^2 and the Gaussian shapes.

of average power are demonstrated with a slightly longer pulse duration of 173 fs and a spectrum centered at 1049 nm with a spectral bandwidth of 7 nm. We attribute this better performance to the spectral shift from 1046.7 to 1049 nm (Fig. 7). This shift can be caused by two effects: first, by some higher losses in the case of shorter pulses, which tend to increase the saturated gain and thus to blueshift the gain cross section spectra (Fig. 7), and second, by a laser cavity alignment favoring the shortest (respectively, longest) wavelengths. In the case of the longest pulse operation, the pulses are also very close to the theory with a temporal Strehl ratio compared with the ideal flat-phase sech^2 solution by 95% and a time–bandwidth product of 5% above the theoretical one. The ML threshold was observed for a laser average power of 413 mW with the corresponding pulse duration of 217 fs (Fig. 6). At maximum power (6.7 W of

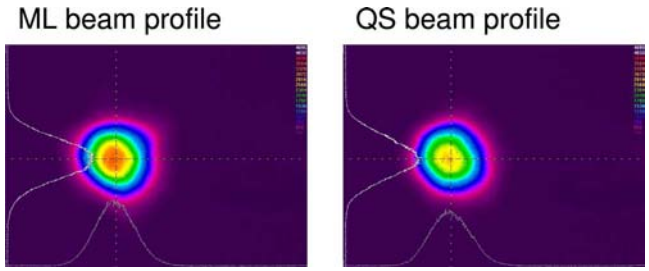

Fig. 5. (Color online) Spatial beam profiles in ML and QS regimes.

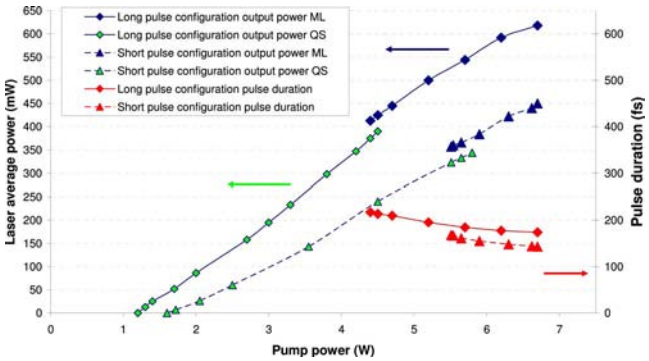

Fig. 6. (Color online) Output average power and pulse duration versus pump power.

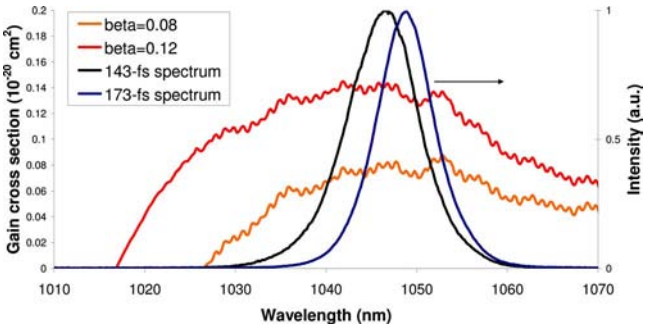

Fig. 7. (Color online) Spectra of the 173 and 143 fs pulses and normalized gain cross sections of Yb:SrF_2 for a typical estimate of β: β=8% and 12%.

emitted pump and 620 mW of laser), the optical–optical efficiency is 9.3%, which is slightly higher than the one obtained with Yb:CaF_2 with a similar setup (595 mW). This is mainly due to the higher absorption of Yb:SrF_2 (higher absorption cross section and higher doping level).

In conclusion, we demonstrated for the first time (to our knowledge) a femtosecond oscillator based on Yb:SrF_2 crystal. The stable mode-locked regime was observed despite the very long lifetime of this crystal. It was mainly ensured by the presence of the SESAM device. As expected, the regime was very close to the solitonlike regime with a temporal Strehl ratio and a time–bandwidth product deviating from the theory by about 5%. Two regimes were observed. The shortest pulse duration was 143 fs for an average power of 450 mW and the maximum average power was 620 mW for a pulse duration of 173 fs. In our cavity, with Yb:SrF_2, the free-running emission is around 1049 nm, which is blueshifted compared with the one corresponding to Yb:CaF_2 (around 1053 nm in a similar setup). According to the smoother spectral gain curves, Yb:SrF_2 has the potential to generate shorter pulses than Yb:CaF_2, but owing to a longer emission lifetime, the stability issue becomes more critical and, even with the same setup, we did not observe shorter pulses with SrF_2. Moreover, probably owing to stability concerns, KLM assisted ML operation was not achieved up to now with Yb:SrF_2. Although Yb:SrF_2 does not compare favorably with Yb:CaF_2 for oscillators in terms of pulse duration and stability, it might be interesting for amplifiers because of its high energy storage capacity and its broad and smooth gain bandwidth.

This work was supported by the CNRS-Mission Ressources et Compétences Technologiques (Cristaux Massifs, Micro-nano-structures et Dispositifs pour l'Optique and réseau technologique femtoseconde LASUR) network [16] through the entitled CRYBLE program.

References

1. A. Lucca, M. Jacquemet, F. Druon, F. Balembois, P. Georges, P. Camy, J. L. Doualan, and R. Moncorgé, Opt. Lett. **29**, 1879 (2004), and references therein.
2. A. Lucca, G. Debourg, M. Jacquemet, F. Druon, F. Balembois, P. Georges, P. Camy, J. L. Doualan, and R. Moncorgé, Opt. Lett. **29**, 2767 (2004).
3. M. Siebold, M. Hornung, R. Boedefeld, S. Podleska, S. Klingebiel, C. Wandt, F. Krausz, S. Karsch, R. Uecker, A. Jochmann, J. Hein, and M. C. Kaluza, Opt. Lett. **33**, 2770 (2008).
4. M. Siebold, M. Hornung, S. Bock, J. Hein, M. C. Kaluza, J. Wemans, and R. Uecker, Appl. Phys. B **89**, 543 (2007).
5. C. R. A. Catlow, A. V. Chadwick, G. N. Greaves, and L. M. Moroney, Nature **312**, 601 (1984).
6. J. Boudeile, J. Didierjean, P. Camy, J. L. Doualan, A. Benayad, V. Ménard, R. Moncorgé, F. Druon, F. Balembois, and P. Georges, Opt. Express **16**, 10098 (2008).
7. S. Chénais, F. Druon, S. Forget, F. Balembois, and P. Georges, Prog. Quantum Electron. **30**, 89 (2006).
8. P. Camy, J. L. Doualan, A. Benayad, M. von Edlinger, V. Ménard, and R. Moncorgé, Appl. Phys. B **89**, 539 (2007).
9. V. Petit, P. Camy, J.-L. Doualan, X. Portier, and R. Moncorgé, Phys. Rev. B **78**, 085131 (2008).
10. M. Siebold, J. Hein, M. C. Kaluza, and R. Uecker, Opt. Lett. **32**, 1818 (2007).
11. C. Hönninger, R. Paschotta, F. Morier-Genoud, M. Moser, and U. Keller, J. Opt. Soc. Am. B **16**, 46 (1999).
12. F. Friebel, F. Druon, J. Boudeile, D. N. Papadopoulos, M. Hanna, P. Georges, P. Camy, J. L. Doualan, A. Benayad, R. Moncorgé, C. Cassagne, and G. Boudebs, Opt. Lett. **34**, 1474 (2009).
13. F. X. Kärtner and U. Keller, Opt. Lett. **20**, 16 (1995).
14. U. Keller, in *Nonlinear Optics in Semiconductors II*, A. Kost and E. Garmire, eds., Vol. 59 of Semiconductors and Semimetals (Academic, 1999), pp. 211–286.
15. H. A. Haus, J. Appl. Phys. **46**, 3049 (1975).
16. http://www.mrct.cnrs.fr/reseaux.htm.